© 2020. Published by The Company of Biologists Ltd | Development (2020) 147, dev181263. doi:10.1242/dev.181263

HUMAN DEVELOPMENT

RESEARCH ARTICLE

Low oxygen enhances trophoblast column growth by potentiating differentiation of the extravillous lineage and promoting LOX activity

Jenna Treissman[1,2], Victor Yuan[1,3], Jennet Baltayeva[1,2], Hoa T. Le[1,2], Barbara Castellana[1,2], Wendy P. Robinson[1,3] and Alexander G. Beristain[1,2,*]

ABSTRACT

Early placental development and the establishment of the invasive trophoblast lineage take place within a low oxygen environment. However, conflicting and inconsistent findings have obscured the role of oxygen in regulating invasive trophoblast differentiation. In this study, the effect of hypoxic, normoxic and atmospheric oxygen on invasive extravillous pathway progression was examined using a human placental explant model. Here, we show that exposure to low oxygen enhances extravillous column outgrowth and promotes the expression of genes that align with extravillous trophoblast (EVT) lineage commitment. By contrast, supra-physiological atmospheric levels of oxygen promote trophoblast proliferation while simultaneously stalling EVT progression. Low oxygen-induced EVT differentiation coincided with elevated transcriptomic levels of lysyl oxidase (*LOX*) in trophoblast anchoring columns, in which functional experiments established a role for LOX activity in promoting EVT column outgrowth. The findings of this work support a role for low oxygen in potentiating the differentiation of trophoblasts along the extravillous pathway. In addition, these findings generate insight into new molecular processes controlled by oxygen during early placental development.

KEY WORDS: Hypoxia, Placentation, Trophoblast, Extravillous trophoblast, Villous cytotrophoblast, Lysyl oxidase, Human

INTRODUCTION

In mammalian development, the placenta forms the mechanical and physiological link between maternal and fetal circulations. In rodents and humans, which have invasive haemochorial placentae, nutrient and oxygen transfer between mother and fetus is achieved through extensive uterine infiltration by placenta-derived cells of epithelial lineage called trophoblasts (Pijnenborg et al., 2011; Velicky et al., 2016). In humans, trophoblast differentiation into invasive cell subtypes, called extravillous trophoblast (EVT), is essential for optimal placental function (Tilburgs et al., 2015a; Velicky et al., 2016). Molecular processes governing invasive EVT differentiation (Haider et al., 2016; Horii et al., 2016; Wakeland et al., 2017) and specific EVT functions such as uterine artery remodelling (Ashton et al., 2005; Keogh et al., 2007) and immunomodulation (Tilburgs et al., 2015a,b) of maternal leukocytes are strictly controlled. Defects in trophoblast differentiation along the EVT pathway are thought to result in impaired placental function and potentially contribute to aberrant conditions of pregnancy that directly impact fetal and maternal health (Avagliano et al., 2012).

In early pregnancy, anchoring villi of the placental basal plate initiate cellular differentiation events leading to the formation of EVT. At specific villi-uterine attachment points, proliferative EVT progenitors establish multi-layered cellular structures called anchoring columns (Haider et al., 2016; Pollheimer et al., 2018). Trophoblasts residing within proximal regions of anchoring columns, termed proximal column trophoblasts (PCT), are highly proliferative and show evidence of initial molecular characteristics that are hallmarks of EVT (Haider et al., 2018; Turco et al., 2018). At distal regions within anchoring columns, column trophoblasts lose their proliferative phenotype and express many markers akin to invasive EVT, such as human leukocyte antigen G (HLA-G), α5 and β1 integrins, NOTCH2 and ERBB2 (Fock et al., 2015a,b; Haider et al., 2016; Kabir-Salmani et al., 2004; Zhou et al., 1997). The transition of PCT into distal column trophoblasts (DCT) represents a significant developmental step towards the formation of uterine-invading and tissue-remodelling EVT.

Anchoring columns of the placenta initially develop in the absence of maternal blood and, subsequently, within a relatively low oxygen environment (~20 mmHg) (Jauniaux et al., 2000; Jauniaux et al., 1999; Rodesch et al., 1992). By comparison, the partial pressure of arterial blood oxygen is ~100 mmHg, whereas the partial pressure of oxygen within the placental bed by 14 weeks' gestation is estimated to be between 40 mmHg and 60 mmHg (Jauniaux et al., 2001). The role of oxygen in controlling anchoring column formation and EVT differentiation has been the focus of many studies (Caniggia et al., 2000; Genbacev et al., 1997; James et al., 2006; Lash et al., 2006; Wakeland et al., 2017). Unfortunately, contradictory and inconsistent findings have obscured the role of oxygen tension in controlling aspects of trophoblast biology, in which low oxygen both promotes (Caniggia et al., 2000; Genbacev et al., 1997) and restrains (James et al., 2006; Lash et al., 2006) column outgrowth, and potentiates (Wakeland et al., 2017) and inhibits (Caniggia et al., 2000; Genbacev et al., 1997) EVT differentiation. These reported differences on the effect of oxygen on anchoring column outgrowth and EVT differentiation are likely attributed to differences in model platforms and methods used to isolate, characterize and culture trophoblasts. Nonetheless, the role of oxygen in controlling anchoring column formation and column trophoblast differentiation has yet to be fully examined.

In this study, we examine how differing levels of oxygen affect first trimester placental column outgrowth. Using placental villous

[1]The British Columbia Children's Hospital Research Institute, Vancouver V5Z 4H4, Canada. [2]Department of Obstetrics & Gynecology, The University of British Columbia, Vancouver V5Z 4H4, Canada. [3]Department of Medical Genetics, The University of British Columbia, Vancouver V5Z 4H4, Canada.

*Author for correspondence (aberista@mail.ubc.ca)

W.P.R., 0000-0002-2010-6174; A.G.B., 0000-0002-1117-6242

Received 12 June 2019; Accepted 18 December 2019

Development (2020) 147, dev181263. doi:10.1242/dev.181263

tissue explants that recapitulate many of the morphological and molecular events central to anchoring column formation and EVT differentiation *in vivo*, we show that low levels of oxygen potentiate column outgrowth. We demonstrate that low oxygen drives hypoxia-related gene programmes and processes that are central to cell-extracellular matrix (ECM) interaction, whereas exposure to high oxygen promotes/maintains a strong proliferative phenotype. Moreover, we provide evidence that supports a role for low levels of oxygen in promoting the differentiation of column trophoblasts along the EVT pathway. We further identify *LOX* as a crucial gene upregulated in response to low oxygen that supports column outgrowth, and provide important insight into novel molecular programmes impacted by oxygen that align with trophoblast differentiation along the EVT pathway.

RESULTS

Hypoxia potentiates trophoblast column outgrowth

To test the effect of exposure to differing levels of oxygen on trophoblast column establishment and outgrowth, we utilized a Matrigel-embedded placental explant model that closely reproduces developmental processes of trophoblast column cell expansion and differentiation along the EVT pathway (Bilban et al., 2009; Newby et al., 2005). Early column formation during human placental development is characterized by the expansion of mitotically active $Ki67^{+}$/$HLA\text{-}G^{lo}$ PCTs into $HLA\text{-}G^{hi}$ non-proliferating DCTs and invasive EVT (Fig. 1A,B). To this end, Matrigel-embedded placental explants recapitulate anchoring column cell organization and EVT-lineage commitment, establishing the explant system as an appropriate experimental tool to study the cellular and molecular underpinnings regulating human trophoblast column formation and outgrowth (Fig. 1C).

Chorionic villi harvested from early first trimester placentae (n=8; 5-8 weeks' gestation) were embedded into Matrigel matrix and allowed to establish for 24 h at 5% oxygen (Fig. 2A); this level of oxygen represents a relative 'normoxic' condition for early placental development (Jauniaux et al., 2001). Characteristics (age, gestational age, BMI, smoking status) of each patient who donated their placenta for explant culture are listed in Table S1. Following this, explants derived from the same placenta were transferred into one of three conditions for an additional 48 h representing either hypoxic (1%, ~10 mmHg O_2), normoxic (5%, ~35 mmHg O_2) or hyperoxic (20%, ~141 mmHg O_2) environments relative to the first trimester of pregnancy (Fig. 2A). Within all oxygen conditions, explant outgrowth was observed (Fig. 2B,C). However, column outgrowth was most pronounced in 1% and 5% oxygen, where outgrowth area in both of these low oxygen conditions was significantly greater than outgrowth observed in 20% oxygen (Fig. 2C,D). Although column outgrowth in 5% oxygen was overall less variable and trended on producing smaller columns than explants cultured in 1% oxygen, there was no statistical difference between outgrowth in 1% and 5% oxygen (Fig. 2D). To account for the possibility that differing oxygen levels may influence column outgrowth by affecting explant cell viability, we assessed trophoblast apoptosis within explant columns and matrix-invading EVT in a subset of the placental explants described above (n=4). Although a detectable cleaved caspase 3 signal was evident within the mesenchymal core of all explants, differing levels of oxygen did not associate with differences in cleaved caspase 3 rates within columns or EVT (Fig. 2E). This finding indicates that outgrowth differences related to oxygen level are likely not the result of heightened/decreased cell apoptosis/viability (Fig. 2E,F). In summary, trophoblast column outgrowth was potentiated by low

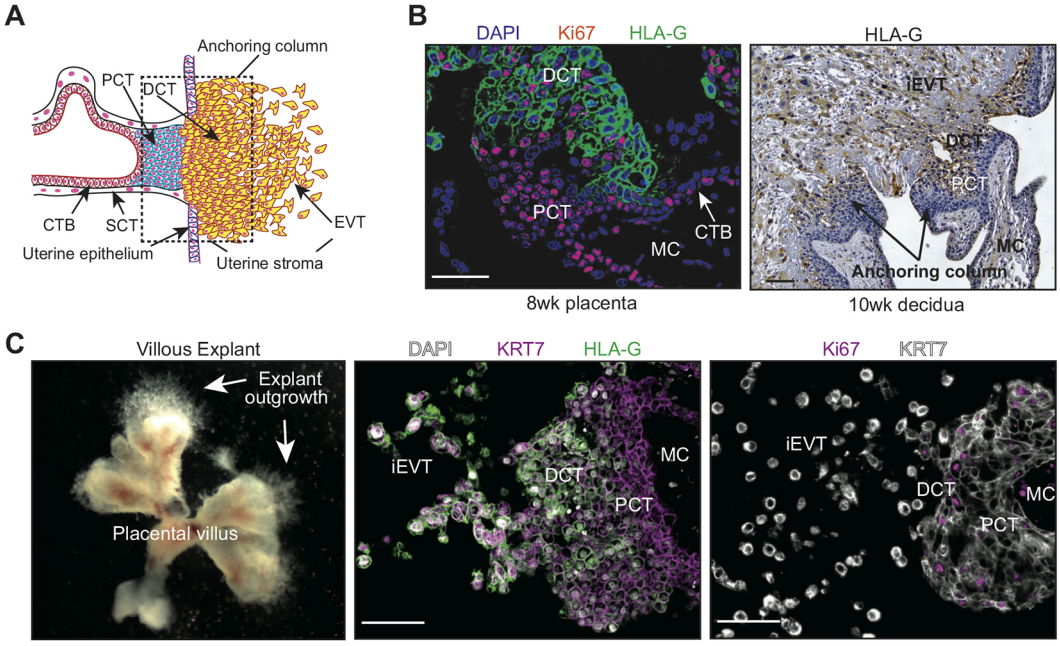

Fig. 1. Establishment of a human placental villous explant model. (A) Schematic showing trophoblast subtypes within placental villus, anchoring column and maternal uterine tissue. Depicted are villous cytotrophoblast (CTB), syncytiotrophoblast (SCT), proximal column trophoblast (PCT) and distal column trophoblast (DCT), and invasive interstitial and endovascular extravillous trophoblast (EVT). (B) Immunofluorescence and immunohistochemistry images showing Ki67 (red) and HLA-G (green, brown) expression in human first trimester placental (8 weeks' gestation) and decidual (10 weeks' gestation) tissues. Shown are CTB (arrow, left panel), PCT and DCT, interstitial EVT (iEVT) and the mesenchymal core (MC). Arrows in the right panel indicate anchoring columns. (C) Images showing gross villous explant establishment and outgrowth (arrows) as well as localization of KRT7 (magenta; white), HLA-G (green) and Ki67 (magenta) to specific subtypes of trophoblasts within explant columns. Nuclei are shown via DAPI staining (white). Scale bars: 100 µm (200 µm in C, left).

Development (2020) 147, dev181263. doi:10.1242/dev.181263

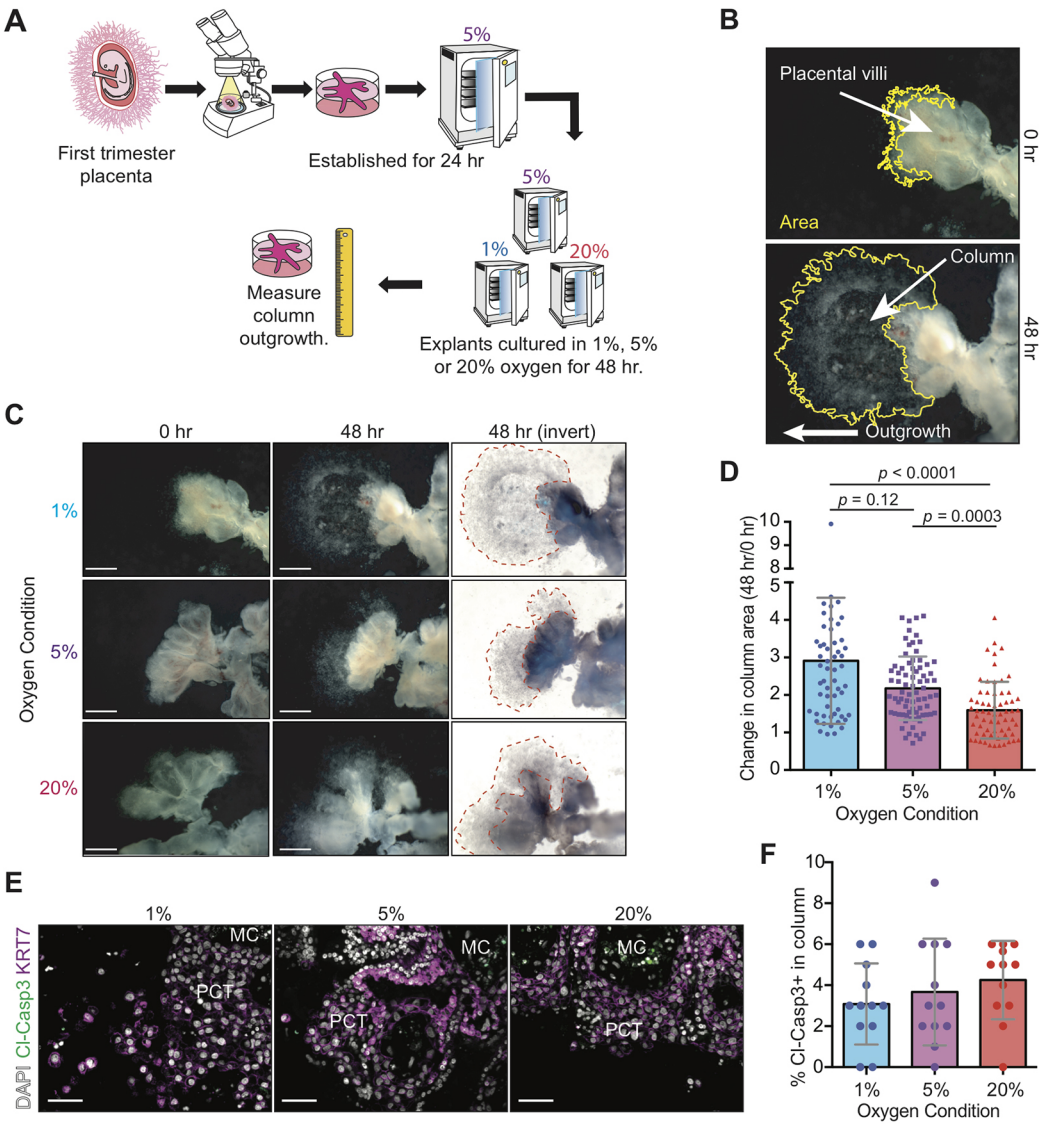

Fig. 2. Exposure to low oxygen promotes trophoblast column outgrowth. (A) Schematic depicting the experimental approach to establishing and culturing placental explants in 1%, 5% and 20% oxygen. (B) Representative images showing how explant column outgrowth area is measured at 0 h and 48 h of culture. The direction of explant outgrowth/invasion is also indicated (horizontal arrow). (C) Representative images of villous explants (n=8 distinct placentae; multiple explants per placenta) cultured in 1%, 5% and 20% oxygen. Shown within the inverted (invert) image is the area of column outgrowth (red dashed line) at 48 h of culture. (D) Bar with scatter plots showing the fold-change of column outgrowth between 48 h and 0 h of exposure to 1%, 5% or 20% oxygen. (E) Immunofluorescence images showing cleaved caspase 3 (green), KRT7 (magenta) and DAPI (white) in placental explants (n=4 distinct placentae; multiple explants per placenta) cultured in 1%, 5% and 20% oxygen for 48 h. Shown is the mesenchymal core (MC) and trophoblasts of the proximal column (PCT). (F) Bar with scatter plots showing the proportion of column trophoblasts staining positive for cleaved caspase 3. Data are median±s.d. Statistical analyses between groups were performed using ANOVA and two-tailed Dunn's post-test; differences significant at P<0.05. Scale bars: 100 µm in E; 200 µm in B,C.

oxygen, whereas exposure to atmospheric oxygen (20% oxygen) blunted column outgrowth.

Explant exposure to low or high levels of oxygen generate distinct transcriptomic signatures

To gain mechanistic insight into how hypoxic, physiologically normal and high levels of oxygen modulate trophoblast column outgrowth, global gene expression was analyzed in placental explant cultures using gene microarrays. For this experiment, placental explants from five unique placentae (n=5; 5-7 weeks' gestation) were established as previously described, except that cultures were maintained in their respective oxygen condition (1%, 5% or 20%) for 24 h before RNA isolation in order to capture molecular signatures central to column formation. Following an approach described within Bilban et al. (2009), chorionic villi of explants were carefully micro-dissected away from columns and EVT and RNA was extracted from only column trophoblasts and Matrigel-invading EVT (Fig. 3A); little or no evidence of outgrowth contributed by vimentin-positive mesenchymal cells was observed (Fig. S1A,B). Following standard probe filtering, and normalization (Fig. S1C-F), differential gene expression (DGE) analysis of explant trophoblasts was performed. Using a false discovery rate (FDR)<0.05, we identified many differences in gene expression between 1% versus 20% (293 genes upregulated; 685 genes downregulated) and 5% versus 20% (363 genes upregulated; 406 genes downregulated) oxygen conditions (Fig. 3B; Table S2). DGE analysis between 1% and 5% oxygen did not identify differentially expressed genes (Fig. 3B). Principal component analysis (PCA)

Development (2020) 147, dev181263. doi:10.1242/dev.181263

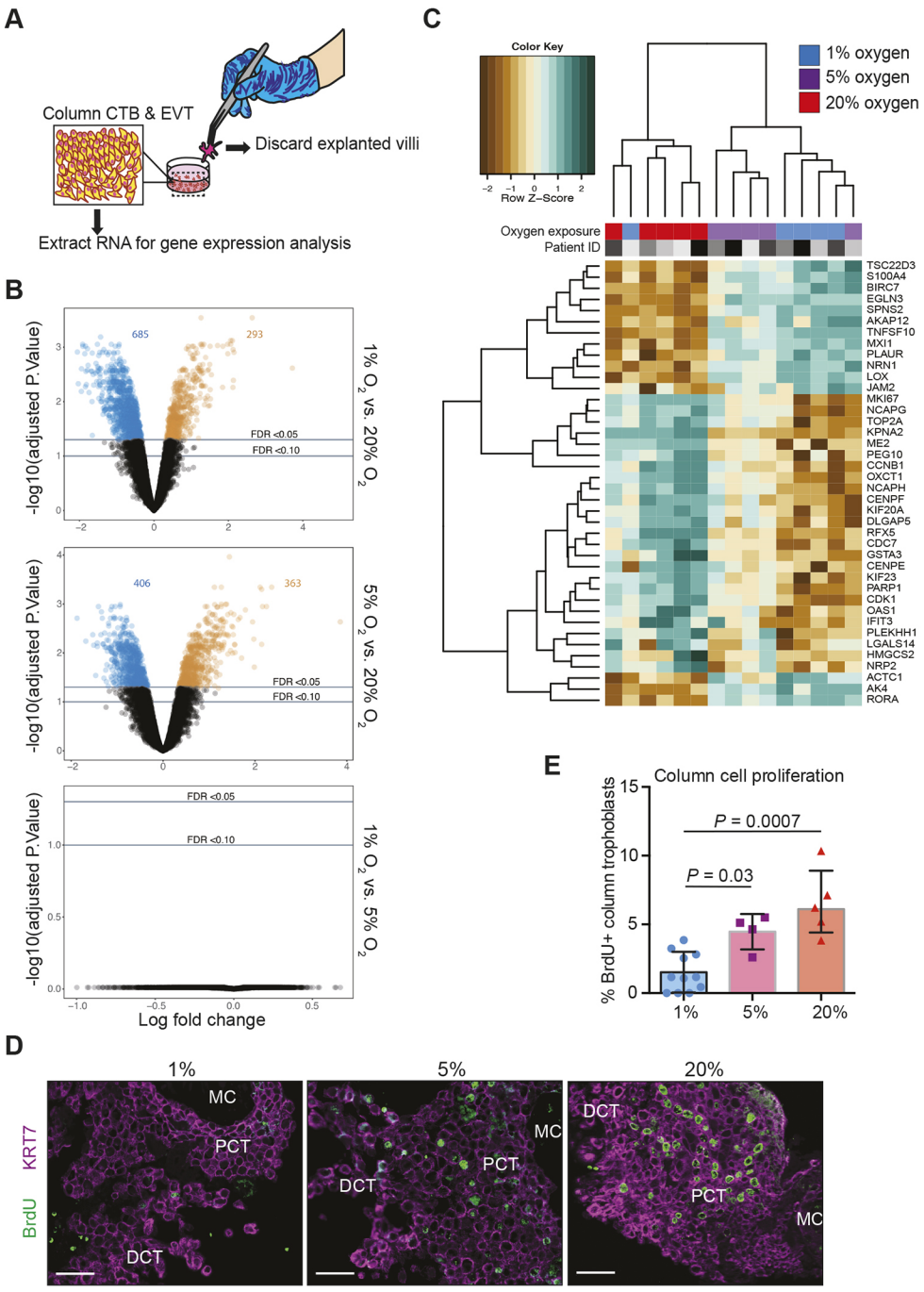

Fig. 3. Comparison of global gene expression patterns between trophoblast columns exposed to 1%, 5% and 20% oxygen. (A) Schematic highlighting the removal of placental villi and retention of column trophoblasts and invasive EVT for gene expression analysis. (B) Volcano plots showing individual gene-targeting probes differentially expressed between 1% and 20%, 5% and 20%, and 1% and 5% oxygen cultures. *x*-axis: coefficients from linear model in log2 scale; *y*-axis: negative log base 10 of the false discovery rate (FDR). Black circles indicate probes with an FDR>0.05; blue and orange circles indicate underexpressed and overexpressed probes with an FDR<0.05, respectively. (C) Dendrogram depicts hierarchical clustering of 1%, 5% and 20% oxygen cultured column trophoblasts using *z*-scores from the top 40 differentially expressed genes from 1% versus 20% comparisons; n=5 per oxygen group. Within the heatmap: brown, low expression; white, mid-level expression; green, high expression. For each sample, oxygen condition (1%, blue; 5%, purple; 20%, red) is indicated, as is the unique placental sample/patient ID used to generate the explant (indicated by shade of grey). (D) Representative immunofluorescence images of BrdU signal (green) within placental explant columns cultured in 1%, 5% or 20% oxygen. Trophoblasts are identified by KRT7 signal (magenta). (E) Bar with scatter plots showing quantification of BrdU incorporation into column trophoblasts cultured in 1%, 5% or 20% oxygen. Data are median±s.d. Statistical analyses between groups were performed using ANOVA and two-tailed Tukey post-test; differences significant at P<0.05. DCT, distal column trophoblast; MC, mesenchymal core; PCT, proximal column trophoblast. Scale bars: 100 µm.

shows clustering of explants cultured in hypoxic, normoxic and hyperoxic conditions (Fig. S2). PCA sample clustering showed explant trophoblasts cultured in 1% and 5% oxygen generally clustered closer together, save for two 1% oxygen explant outliers; one clustered among 20% oxygen samples whereas the other clustered separately to all other samples (Fig. S2). Despite these two explants being identified as significant outliers using the Silhouette coefficient (Barghash and Arslan, 2016), we opted to retain them for the remainder of our analyses as we could not confidently ascribe outlier classification owing to technical or batch-related artefacts.

Hierarchical clustering of the 15 column trophoblast samples segregated samples into two statistically significant clusters (sigclust, P<0.05): a 20% oxygen-dominated cluster and a cluster composed of column trophoblasts cultured in 1% and 5% oxygen (Fig. 3C). A gene heat-map of the top 40 differentially expressed genes (top 20 differentially expressed genes in 1%; top 20 differentially expressed genes in 20%; FDR<0.05, ranked by fold change) highlights gene patterns across 1%, 5% and 20% oxygen cultures (Fig. 3C). In both 1% and 5% oxygen conditions, the top hits identified by global DGE analysis included genes associated with hypoxia (*EGLN3*, *RORA*), cell-matrix interaction and/or re-structuring (*LOX*, *JAM2*, *EGLN3*, *PLAUR*) and gene transcription regulation (*MXI1*, *TSC22D3*, *RORA*). In contrast, the most highly expressed genes in explants exposed to 20% oxygen were exclusive to pro-mitotic/proliferative processes (*MKI67*, *KIF20A*, *KIF23*, *PEG10*, *CDK1*, *NCAPG*, *NCAPH*, *TOP2A*, *CDC7*), indicating that column trophoblasts cultured in 20% oxygen possess a proliferative phenotype.

Development (2020) 147, dev181263. doi:10.1242/dev.181263

Differing oxygen levels drive distinct molecular programmes in trophoblast columns

To broadly examine how transcriptomic differences within column trophoblasts exposed to hypoxic, normoxic and hyperoxic conditions relate to differences in molecular pathways, gene signatures determined by DGE analysis (FDR<0.05; fold-change>1.5; Table S2) were used to identify pathways enriched in explant column trophoblasts cultured in 1%, 5% and 20% oxygen. Unsurprisingly, pathways in explants cultured in 1% oxygen (293 genes; clusterProfiler) showed enrichment for multiple pathways and molecular processes specific to hypoxia (Fig. S2C). This finding suggests that placental explants have intact oxygen sensing machinery, and this was confirmed in a separate cohort of explants showing that low oxygen culture (1%) induces a robust hypoxia signal within column cells and EVT compared with explants cultured in atmospheric (20%) conditions (Fig. S2B). The 1% oxygen signature also showed enrichment for pathways related to ECM structure and organization, steroid hormone responses and hydroxyproline metabolism (Fig. S2C). Similar to the 1% oxygen pathway readouts, the 5% oxygen signature (363 genes) showed enrichment for genes specific to ECM composition, response to hypoxia and response to steroid hormones, but also showed enrichment of pathways related to bone development and viral entry into cells (Fig. S2D). By contrast, 20% oxygen (685 genes) showed enrichment of pathways and cellular processes related to organelle fission, nuclear division, chromosome segregation, mitotic nuclear division, and DNA packaging and replication, all of which link to heightened cell cycle activity and proliferation (Fig. S2E).

Using the Mitotic Nuclear Division, Chromosome Segregation and DNA Replication curated gene ontology (GO) gene signatures enriched within 20% column trophoblasts (93 genes; Table S3), explant samples were subjected to hierarchical clustering and visualized by gene heat-map (Fig. S3). Notably, samples segregated into two groups: one group was defined by 1% oxygen samples (4/5 1% oxygen samples) and the other group consisted mostly of 5% and 20% oxygen samples (10/10 5%/20% samples) (Fig. S3). This later branch was further divided into two sub-branches, one enriched by 5% oxygen samples also containing a 1% oxygen sample outlier, and the other sub-branch made up entirely of 20% oxygen column trophoblasts (Fig. S3). Interestingly, gene heat-map expression intensities suggest a step-wise increase in expression of pro-mitotic/proliferative genes in column trophoblasts exposed to increasing levels of oxygen (Fig. S3). To verify whether an increase in exposure to oxygen tension translates into increased proliferation, a BrdU pulse-chase was performed on a separate cohort of placental explants (n=3) cultured in 1%, 5% and 20% oxygen. In support of the gene array data, little or no evidence of cell proliferation within explant columns was observed in 1% oxygen cultures following a 4 h chase (Fig. 3D,E). However, explants cultured in 5% oxygen showed a significant increase in BrdU incorporation within column trophoblasts compared with 1% oxygen columns, and an even greater level of BrdU positivity was measured within 20% oxygen columns (20% versus 1%) (Fig. 3D,E). Though a trend for greater proliferation in explant columns cultured in 20% oxygen compared with 5% oxygen was observed, this difference was not significant (Fig. 3E). Overall, our findings suggest that explant column trophoblasts cultured in low oxygen upregulate molecular processes related to hypoxia/hypoxia inducible factor 1A (HIF1A) signalling and ECM organization/remodelling, whereas column trophoblasts exposed to hyper-physiological 20% oxygen adopt a predominantly pro-proliferative phenotype.

Low oxygen promotes EVT differentiation

Differentiation of trophoblasts along the EVT pathway is in part defined by the exiting of PCT located at the base of anchoring columns from the cell cycle (Velicky et al., 2018). Moreover, as column trophoblasts located at distal portions of columns acquire pro-invasive EVT-like characteristics, molecular pathways related to ECM-remodelling and protease functions are accordingly upregulated (E. Davies et al., 2016). Our observation that low oxygen (1% and 5%) promotes transcriptional signatures linked to cell-ECM interaction and protease-ECM remodelling, whereas 20% oxygen promotes proliferation, suggests that exposure to low oxygen drives, whereas high oxygen restrains, EVT differentiation.

To examine how global gene expression changes identified within low and high oxygen-exposed explants relate to trophoblast differentiation, we examined the expression of the top 15 upregulated genes in column trophoblasts cultured in 1% and 20% oxygen (FDR<0.05; fold-change>2) within a recently reported first trimester placenta single cell transcriptomic dataset (Vento-Tormo et al., 2018). Using this dataset we focused exclusively on the five subtypes of trophoblasts that were described (14,366 trophoblasts from five individual placentae): cytotrophoblast (CTB), proliferative CTB, syncytiotrophoblast (SCT), proliferative EVT (likely PCT) and EVT (likely an admixture of DCT and invasive EVT) (Fig. S4A) (Vento-Tormo et al., 2018). Within uniform manifold approximation and projection (UMAP)-directed cell clusters, the specificity of each trophoblast sub-lineage/type is shown by expression levels of *EGFR* (CTB), *ERVFRD-1* (syncytin-2; SCT), *HLA-G* (column trophoblast and EVT) and *MKI67* (proliferating trophoblast) (Fig. S4B).

To determine whether our 1% and 20% oxygen-dependent genes are more expressed in the EVTs or CTBs, we applied a pseudotime trajectory analysis using a gene signature derived from the top 1000 variable genes within the single cell (sc)RNA-seq dataset. This reproduced a lineage trajectory similar to that reported in Vento-Tormo et al. (2018), in which a predicted cell origin state was identified as well as the two differentiation trajectories aligning with the villous and extravillous pathways (Fig. 4A,B). Correlating trophoblast lineage trajectory with the top upregulated genes identified in the gene array in 1% and 20% oxygen conditions showed that the top fifteen genes enriched within 20% oxygen aligned to both the villous and extravillous pathway trajectories (Fig. 4C). Notably, high-oxygen genes primarily aligned with immature/early EVT and CTB cell states (Fig. 4C). By contrast, the top fifteen low oxygen enriched genes primarily aligned with the fully differentiated stage of the extravillous pathway (i.e. *TNFSF10*, *LOX*, *SPNS2*, *S100A4*, *JAM2*, *PLAUR*) (Fig. 4C). Together, these data suggest that column trophoblasts exposed to low oxygen adopt transcriptomic signatures that are reflective of EVT, whereas column trophoblasts cultured in 20% oxygen express genes that align predominately with the villous pathway and less-advanced states of EVT differentiation.

LOX expression and activity is potentiated by low oxygen

Our finding that low oxygen drives column outgrowth and potentiates the expression of genes linked with the EVT phenotype suggests that genes highly expressed within low oxygen columns may in part contribute to EVT differentiation and/or trophoblast column formation. Rank ordering of upregulated genes by fold-change in both 1% and 5% oxygen column trophoblasts identified multiple conserved genes between the two oxygen conditions (Table S2). Notably, *LOX*, the gene encoding lysyl oxidase, a copper-dependent enzyme that catalyzes collagen and elastin crosslinking, was the

Development (2020) 147, dev181263. doi:10.1242/dev.181263

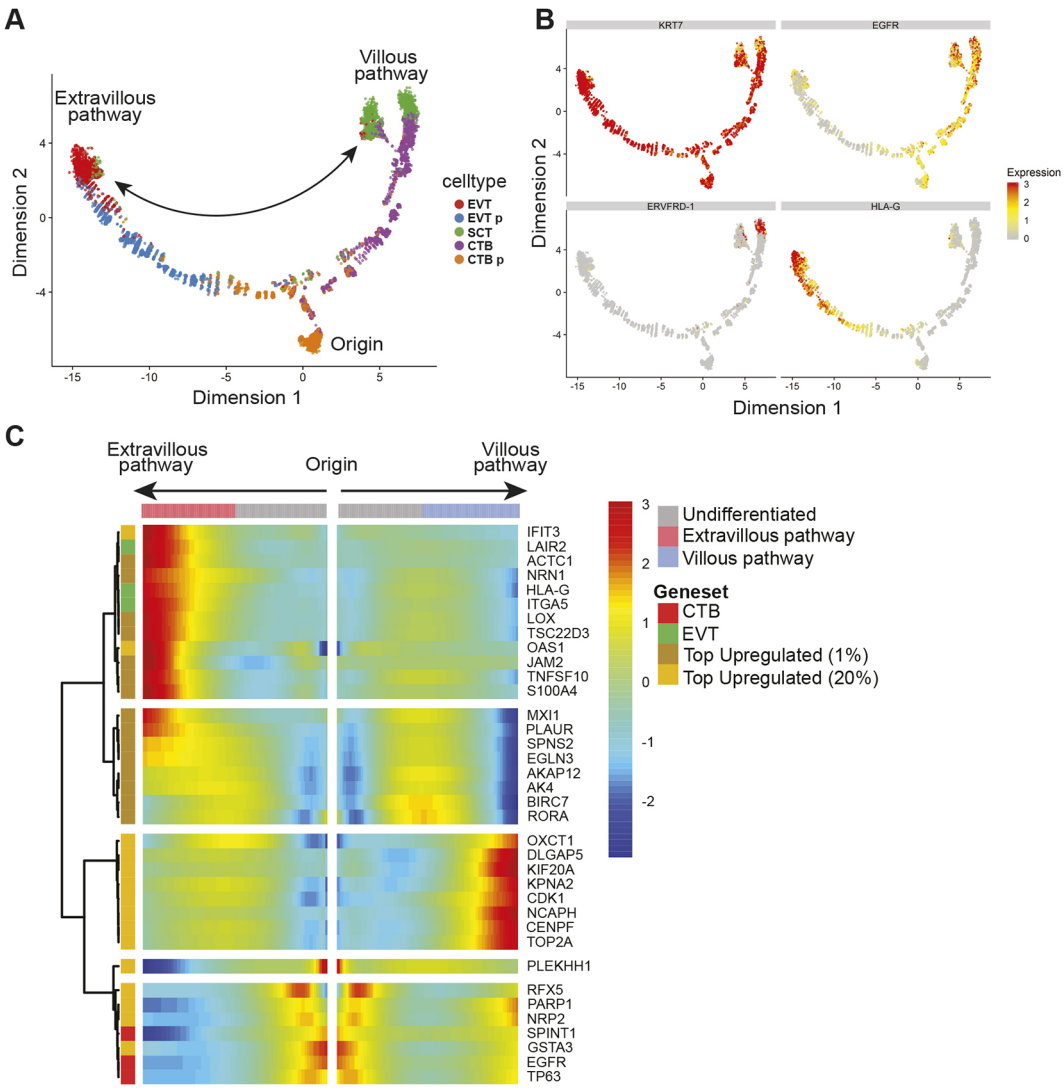

Fig. 4. Low oxygen drives column cell differentiation along the EVT pathway. (A) Pseudotime analysis was applied using Monocle 2 (Qiu et al., 2017; Trapnell et al., 2014) to visualize gene expression across trophoblast differentiation. Two lineage trajectories were identified corresponding to the extravillous pathway and villous pathway (arrow). A cell state of origin is also shown. (B) The inferred trajectory resulted in two distinct endpoints: one branch leading to cells highly expressing the syncytiotrophoblast (SCT) marker (e.g. ERVFRD-1), and another leading to cells highly expressing the extravillous trophoblast (EVT) marker (HLA-G). Also shown within the pseudotime trajectory are the pan-trophoblast marker KRT7 and cytotrophoblast (CTB) marker EGFR. (C) A heatmap was constructed using inferred pseudotime and the top 15 upregulated genes in explants cultured in 1% and in 20% oxygen. Included within the heatmap are known genes that align with the CTB (*EGFR*, *SPINT1*, *TP63*) and EVT (*HLA-G*, *ITGA-5*, *LAIR2*) states. Pseudotime was ordered such that the left and right ends represent the EVT and SCT endpoints. Hierarchical clustering was applied to the genes (ordered along the rows) and separated into five clusters.

number 2-ranked gene in both 1% and 5% oxygen cultured explants. Specifically, *LOX* expression was 6.2- and 5.1-fold higher in 1% and 5% oxygen cultures compared with 20% oxygen explants (Fig. 5A; Table S2). Although previous work has identified a role for elevated *LOX* expression in promoting tumour cell metastasis (Cox et al., 2015; Di Stefano et al., 2016), the role of LOX in placental trophoblast column biology and trophoblast differentiation along the EVT pathway has not been described.

As an initial step to examine the importance of LOX in anchoring column biology, *LOX* mRNA *in situ* hybridization within first trimester placental villi (n=3; 6-8 weeks' gestation) was performed. RNAscope *in situ* hybridization showed specific and intense *LOX* localization to cells within the mesenchymal core of placental villi and to trophoblasts within anchoring columns (Fig. 5B). Little or no *LOX* signal was detected in CTB or SCT (Fig. 5B). RNAscope analysis of *LOX* within placental explants cultured in 1% and 20% oxygen supported the gene array finding that *LOX* expression was elevated in column trophoblasts exposed to low oxygen (Fig. 5C). Immunoblot analysis of protein lysates obtained from column trophoblasts cultured in 1% or 20% oxygen further supported our previous finding that LOX expression is elevated in trophoblasts of anchoring columns exposed to low levels of oxygen (Fig. 5D). Moreover, LOX enzymatic activity measured in conditioned media (CM) generated by placental explants cultured in 1% or 20% oxygen was significantly higher in 1% cultures than in 20% cultures (Fig. 5E). Use of the LOX inhibitor, β-aminopropionitrile (BAPN), demonstrated LOX-substrate specificity, whereas recombinant active LOX served as a positive control (Fig. 5E). Taken together, these findings show that LOX expression and activity is elevated in column trophoblasts cultured in low oxygen. Further, the preferential *in vivo* expression of *LOX* within the trophoblast anchoring column combined with its involvement in promoting tumour cell

Development (2020) 147, dev181263. doi:10.1242/dev.181263

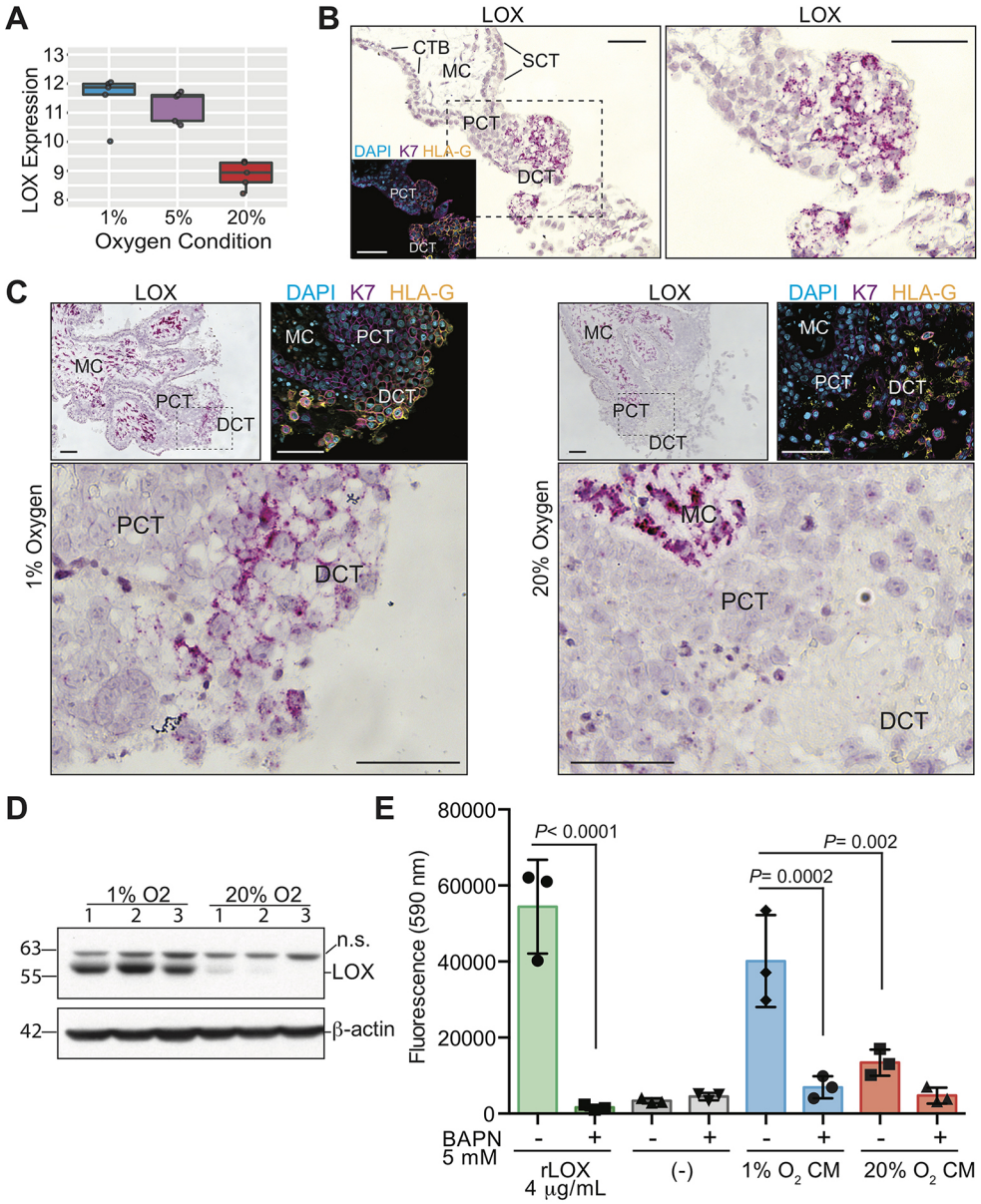

Fig. 5. Low oxygen exposure promotes column-specific expression of *LOX*. (A) Gene array box-plot showing expression levels of *LOX* mRNA in placental explants cultured in 1%, 5% and 20% oxygen. (B) Representative image showing *LOX* mRNA transcript *in situ* localization (dark pink) within a first trimester placental villus. Right panel shows magnification of boxed area in left panel. Shown are annotations of trophoblast/placental subtypes: CTB, cytotrophoblast; DCT; distal column trophoblast; MC, mesenchymal core; PCT, proximal column trophoblast; SCT, syncytiotrophoblast. Inset in left panel shows an immunofluorescent image depicting nuclei (DAPI; blue), keratin-7 (K7; magenta) and HLA-G (orange) localization within a serial section of the same placental villus. (C) Representative images of *LOX* mRNA localization within placental explants cultured in 1% or 20% oxygen. Specific trophoblast subtypes are indicated as above, and the dashed box corresponds to the enlarged area shown below. Also shown are insets of immunofluorescent images depicting nuclei (DAPI; blue), keratin-7 (K7; magenta) and HLA-G (orange) localization within corresponding serial sectioned regions of the explant. (D) Immunoblot showing LOX protein levels in column cells isolated from explants following culture in 1% (n=3) and 20% (n=3) oxygen for 72 h; individual explants are indicated numerically above the blot. n.s. indicates a non-specific band. Molecular weights (kDa) are shown to the left and β-actin indicates loading control. (E) Bar with scatter plots showing LOX activity levels within conditioned media (CM) of placental explants cultured in either 1% or 20% oxygen in the presence or absence of the LOX inhibitor BAPN (5 mM). Recombinant active lysyl oxidase (rLOX) served as a positive control whereas explant culture media alone served as a negative control. Activity corresponds to the level of fluorescence intensity (590 nm). Data are median±s.d. Statistical analyses between groups were performed using ANOVA and two-tailed Tukey post-test; differences significant at P<0.05. Scale bars: 100 µm.

metastasis, suggests that LOX may also play a role in controlling trophoblast column outgrowth and/or EVT differentiation.

Impairment of LOX restrains column outgrowth

To test the function of LOX in column outgrowth, Matrigel-embedded placental explants cultured in 1% and 20% oxygen (n=3 per condition) were cultured in either control explant media or media containing the competitive LOX inhibitor BAPN. The effectiveness of BAPN in inhibiting LOX activity was measured as before by examining the ability of endogenous LOX in explant CM to oxidize substrate (Fig. 6A). CM harvested from control explants showed LOX activity levels slightly below levels measured in

Development (2020) 147, dev181263. doi:10.1242/dev.181263

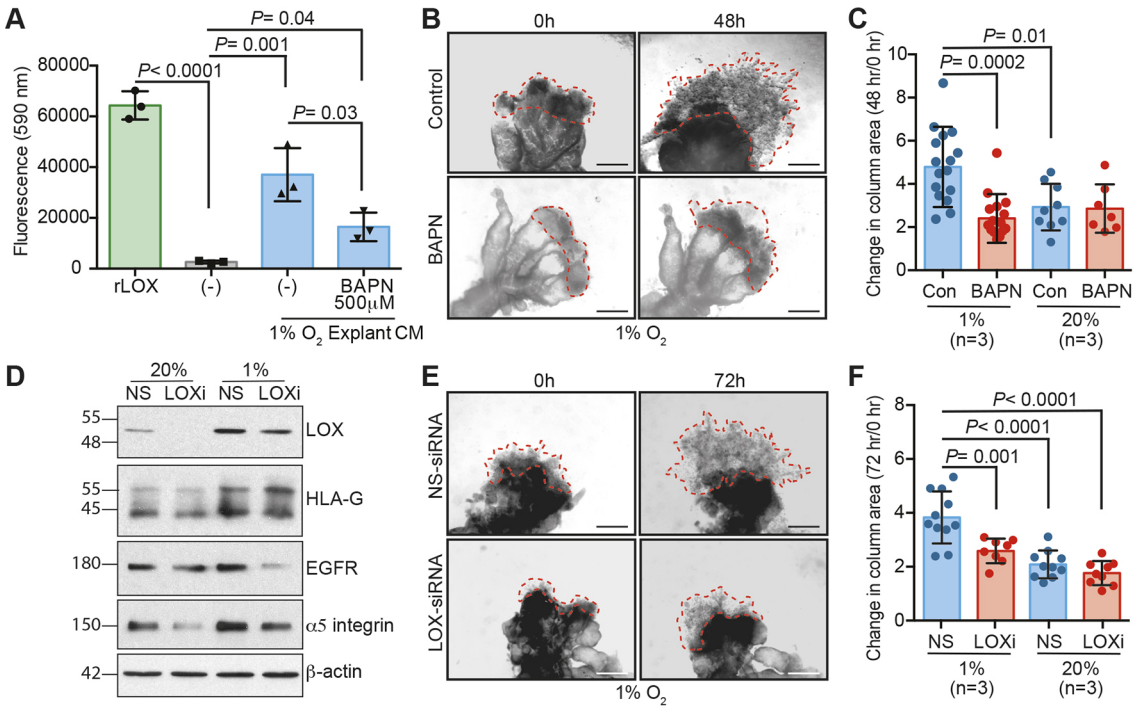

Fig. 6. Inhibition of LOX dampens column outgrowth. (A) Bar with scatter plots showing LOX activity levels within conditioned media (CM) of placental explants cultured in 1% oxygen in the presence or absence of BAPN (500 µM). Recombinant active lysyl oxidase (rLOX) served as a positive control, whereas explant culture media alone served as a negative control. Activity corresponds to level of fluorescence intensity (590 nm). (B) Representative images of villous explants (*n*=3 distinct placentae; multiple explants per placenta) cultured in 1% oxygen and in the presence or absence of BAPN (500 µM). Column outgrowth is shown at 0 h and 48 h of culture (red dashed line). (C) Bar with scatter plots showing the fold-change of column outgrowth between 48 h and 0 h following treatment with BAPN in explants cultured in 1% or 20% oxygen. (D) Representative immunoblots showing LOX, HLA-G, EGFR and α5-integrin protein levels in column cells transfected with non-silencing siRNA (NS) or siRNA targeting LOX (LOXi) isolated from explants following culture in 1% (*n*=3) and 20% (*n*=3) oxygen. Molecular weights (kDa) are shown to the left and β-actin indicates loading control. (E) Representative images of villous explants (*n*=3 distinct placentae; multiple explants per placenta) cultured in 1% oxygen and in the presence of NS or LOXi. Column outgrowth is shown at 0 h and 48 h of culture (red dashed line). (F) Bar with scatter plots showing the fold-change of column outgrowth between 48 h and 0 h following treatment of explants with NS and LOXi siRNA in 1% or 20% oxygen. Data are median±s.d. Statistical analyses between groups were performed using ANOVA and two-tailed Tukey post-test; differences significant at $P<0.05$. Scale bars: 200 µm.

recombinant LOX positive control reactions, but significantly higher than explant media alone (Fig. 6A). Importantly, treatment of explants with BAPN significantly blunted LOX activity, though activity was not completely blocked (Fig. 6A). Treatment with BAPN led to a significant twofold impairment in column outgrowth in explants cultured in 1% oxygen but did not alter outgrowth in explants cultured in 20% oxygen (Fig. 6B,C).

Because BAPN inhibits the activity of LOX as well as the related LOX-like enzymes (i.e. LOXL1-4), of which *LOXL1* expression was also elevated in explants exposed to low oxygen (Table S2), we set out to confirm the specificity of LOX in promoting column outgrowth using LOX-targeting siRNAs. Transient siRNA-directed knockdown in placental explants was confirmed through LOX immunoblotting (Fig. 6D). Although LOX protein levels were low/undetectable in 20% oxygen conditions, baseline (20% oxygen) and hypoxia-driven LOX expression was reduced in LOX-siRNA transfected explants (Fig. 6D). To gain insight into whether LOX impairment may affect EVT differentiation, protein levels of EGFR (a CTB marker), HLA-G and α5-integrin (EVT markers) were examined via immunoblotting. Consistent with our gene array data (Table S2), exposure to low oxygen led to elevated protein levels of EGFR and α5-integrin (Fig. 6D). In addition, explants cultured in 1% oxygen showed higher levels of HLA-G than explants cultured in 20% oxygen, further supporting our findings that low oxygen promotes an EVT phenotype (Fig. 6D). Although LOX knockdown did not result in changes in HLA-G expression, both EGFR and α5-integrin levels were moderately lower in explants exposed to LOX-silencing siRNA (Fig. 6D). Importantly, LOX knockdown led to impaired column outgrowth in placental explants, though the effect of LOX silencing on column outgrowth was less pronounced than BAPN, likely attributed to the less-efficient inhibition of LOX through siRNA silencing (Fig. 6E,F). Taken together, these results suggest that LOX expression in developing trophoblast columns promotes column outgrowth and associates with an EVT phenotype.

DISCUSSION

Here, we describe how exposure to different levels of oxygen differentially affect trophoblast column outgrowth and global gene expression. We provide evidence that exposure to low oxygen results in overall increases in column outgrowth accompanied by gene expression signatures that align with an EVT phenotype. By contrast, gene signatures in high oxygen-cultured column trophoblasts define a role for elevated oxygen in maintaining column growth through cell proliferation. In both hypoxic and normoxic conditions, we identify the gene *LOX* as one of the most highly upregulated genes within explant columns. We show that *LOX* expression associates with EVT lineage trajectory and demonstrate that impairment of LOX activity blunts column outgrowth. Together, this work supports a role for low oxygen in

Development (2020) 147, dev181263. doi:10.1242/dev.181263

potentiating the EVT pathway. Moreover, this work also identifies novel oxygen-sensitive molecular processes that likely play roles in anchoring column formation during human placental development.

The role of oxygen in controlling column formation and the EVT pathway is controversial. Previous studies have shown that exposure of placental explants to low oxygen (i.e. 2% to 3% oxygen) promotes column expansion and outgrowth, with outgrowth primarily attributed to HIF1A-directed cell proliferation (Caniggia et al., 2000; Genbacev et al., 1997). Consistent with this, evidence exists that CTB exposure to low oxygen restrains trophoblast progression along the EVT pathway (Caniggia et al., 2000; Genbacev et al., 1997; Lash et al., 2006). By contrast, rodents and rodent-derived trophoblast stem cells engineered to lack hypoxia-sensing machinery (i.e. *ARNT*, *HIF1A* and/or *EPSA1* null) fail to differentiate into invasive subsets of trophoblasts (Chakraborty et al., 2016, 2011; Cowden Dahl et al., 2005; Gultice et al., 2009; Maltepe et al., 2005). In support of these observations, low oxygen was shown to potentiate an invasive phenotype in human primary trophoblasts with an accompaniment in the expression of EVT-associated genes encoding HLA-G and α5 integrin, and the upregulation of pro-migratory integrin-linked kinase signalling (Horii et al., 2016; Robins et al., 2007; Wakeland et al., 2017). Our findings overall align with these later studies that suggest low oxygen promotes differentiation along the EVT pathway. Notably, we show that low oxygen drives expression of EVT-related genes and signatures that align with EVT lineage trajectory. We show that low oxygen (1% and 5% oxygen) induces expression of hallmark EVT genes such as *ITGA5*, *ADAM12*, and *FLT1*, as well as the transcription factor genes *KLF5* and *GATA3* that are preferentially expressed by EVT. Consistent with this, protein levels of HLA-G and α5 integrin in column trophoblasts exposed to low oxygen were also shown to be elevated. Importantly, the use of cell lineage trajectory modelling using single cell RNA sequencing data provides evidence that low oxygen promotes a cell state consistent with the EVT lineage. These later observations are in line with the association of low levels of oxygen within the intervillous space and anchoring column formation and interstitial EVT infiltration into decidual mucosa in early pregnancy. However, the relationship between relative placental hypoxia and inadequate placentation in aberrant pregnancy conditions such as preeclampsia (Farrell et al., 2019) suggests that the impact of oxygen on trophoblast biology may differ according to stage of development.

Our finding that high levels of oxygen promote column trophoblast proliferation is inconsistent with previous studies investigating the role of hypoxia in anchoring column biology (Caniggia et al., 2000; Genbacev et al., 1997). However, in agreement with our findings, James et al. reported that explant columns cultured in 8% oxygen have increased trophoblast cellularity compared with columns exposed to 1.5% oxygen (James et al., 2006). Moreover, there appears to be consistent agreement that exposure to low oxygen leads to greater column outgrowth, where oxygen tension levels between 1% and 5% consistently generate larger columns than atmospheric oxygen conditions (Caniggia et al., 2000; James et al., 2006). However, dissecting how enhanced column outgrowth is achieved, i.e. via greater cell proliferation within the column or through increased trophoblast migration and invasion, is still not completely resolved. Indeed, although our data suggests that low oxygen promotes an EVT phenotype and enhances molecular pathways related to cell-ECM remodelling, we did not directly examine whether low oxygen affects EVT invasion. Our findings and the findings of others (Wakeland et al., 2017) suggest that low oxygen promotes the differentiation of immature EVT, whereas higher oxygen gradients spur the maturation of terminally differentiated EVT and promote EVT-related processes like cell invasion. Because oxygen gradients *in vivo* are not abrupt, but rather follow a gradual rise in oxygen between the proximal region of the anchoring column to well-vascularized areas of the decidua, previous studies showing a role for elevated levels of oxygen in promoting EVT functions are consistent with the paradigm that low oxygen promotes immature EVT formation whereas higher levels of oxygen complete the EVT differentiation process (Chang et al., 2018). The stark differences on the effect of oxygen levels in regulating trophoblast proliferation within explant columns between various studies is difficult to explain, but may stem from differences in media composition, the matrix substratum used in explant cultures, subtle variations in oxygen tension and the gestational age of placental tissues/cells used for establishing explant cultures. Future studies will need to specifically re-examine how differing levels of oxygen impact column cell proliferation.

Our finding that *LOX* expression was consistently highly upregulated in both 1% and 5% column trophoblasts compared with those cultured in 20% oxygen indicates that LOX-related processes are important in placental development and trophoblast column biology. Although a role of LOX in column formation has not been previously reported, the importance of LOX in tumourigenesis is known, in which elevated LOX associates with numerous types of cancers and LOX activity promotes tumour cell metastasis (Cox et al., 2015; Di Stefano et al., 2016). Further, previous reports do provide evidence that LOX expression is restricted to column trophoblasts (Segond et al., 2013) and promotes cell invasion of a trophoblast cell line (Xu et al., 2019). This later finding is consistent with the association of LOX expression and the EVT phenotype. Aldehydes produced by LOX-directed oxidation of lysine residues within collagen and elastin facilitate collagen/elastin cross-linking and stability, which in turn provide a structural lattice for cell movement (Kim et al., 2014). That *LOX* expression is greatest within both PCT and DCT is interesting, as PCT are not considered to be migratory. Nonetheless, it is likely that creating an appropriate substratum scaffold via LOX-directed collagen crosslinking may contribute to column stability and provide a platform for EVT outgrowth. How or whether LOX affects anchoring column establishment or EVT differentiation was not sufficiently addressed in this study. We provide some evidence that impairment in LOX expression leads to a reduction in α5-integrin, an immature EVT marker; however, LOX silencing also results in reduced EGFR, a CTB marker. Thus, the role of LOX in controlling trophoblast differentiation requires further study, and future work utilizing newly-derived trophoblast organoids (Haider et al., 2018; Turco et al., 2018) and trophoblast stem cells (Okae et al., 2018) will allow for validation of our findings and may allow for deep mechanistic examination of LOX and the EVT pathway.

In summary, the extravillous pathway is controlled by multiple intrinsic as well as extrinsic factors, including the level of oxygen. We provide evidence that supports a role for low oxygen levels in promoting the differentiation of trophoblasts along the EVT pathway. This finding establishes insight into crucial developmental events during placentation that occur in early pregnancy. Further, these findings may also provide a foundation for understanding cellular and molecular processes contributing to conditions linked to aberrant placentation.

Development (2020) 147, dev181263. doi:10.1242/dev.181263

MATERIALS AND METHODS

Patient recruitment and tissue collection

Decidual and placental tissues were obtained with approval from the Research Ethics Board on the use of human subjects, University of British Columbia (H13-00640). All samples were collected from women (19 to 39 years of age) providing written informed consent undergoing elective terminations of pregnancy at British Columbia's Women's Hospital, Vancouver, Canada. First trimester decidual (N=1) and placental tissues (N=38) were collected from participating women (gestational ages ranging from 5 to 12 weeks) having confirmed viable pregnancies by ultrasound-measured fetal heartbeat. The decidual tissue sample was selected based on the presence of a smooth uterine epithelial layer and a textured thick spongy underlayer. Patient clinical characteristics (i.e. height and weight) were also obtained to calculate body mass index (BMI: kg/m^2) and all consenting women provided self-reported information via questionnaire to having first hand exposure to cigarette smoke, and are summarized in Table S1.

Placental villous explant assay

Ex vivo placental villous cultures were established as described in Aghababaei et al. (2014), De Luca et al. (2017) and Perdu et al. (2016). Briefly, placental villi from 5-8 week old gestation placentas (n=8) obtained from patients undergoing elective termination of pregnancy were dissected, washed in ice-cold PBS, and embedded into Millicell cell culture inserts (0.4 µm pores, 12 mm diameter; EMD Millipore) containing 200 µl of growth-factor-reduced Phenol-red free Matrigel (BD Biosciences). Explants, containing 400 µl DMEM/F12 1:1 (200 mM L-glutamine) in the outer chamber, were allowed to establish overnight in a humidified 37°C trigas incubator at 5% oxygen, 5% CO_2. Following 24 h of culture, explants were cultured in 200 µl DMEM/F12 1:1 media and placed into 1%, 5% or 20% oxygen incubators for either an additional 24 h (gene expression analyses) or 48 h (explant outgrowth measurements). All explant media were supplemented with penicillin/streptomycin and antimycotic solution (Thermo Fisher Scientific). Growing explants were imaged at indicated times using a Nikon SMZ 7454T triocular dissecting microscope outfitted with a digital camera. EVT outgrowths were measured using ImageJ software. Fold-change in outgrowth was determined by dividing the mean column area at 48 h into the mean area at 0 h.

Immunofluorescence, RNAScope and immunohistochemistry microscopy

Immunofluorescence

Placental villi (6-12 weeks' gestation; n=5) or placental explants (derived from n=16 placentae) were fixed in 2% paraformaldehyde overnight at 4°C. Tissues were paraffin embedded and sectioned at 6 µm onto glass slides. Immunofluorescence was performed as described elsewhere (Aghababaei et al., 2015). Briefly, cells or placental tissues underwent antigen retrieval by heating slides in a microwave for 5×2 min intervals in a citrate buffer (pH 6.0). Sections were incubated with sodium borohydride for 5 min at room temperature (RT), followed by Triton X-100 permeabilization for 5 min at RT. Slides were blocked in 5% normal goat serum/0.1% saponin for 1 h at RT, and incubated with combinations of the indicated antibodies overnight at 4°C: anti-HLA-G (1:100, 4H84, Exbio); anti-cytokeratin 7, mouse monoclonal IgG (1:50, RCK105, Santa Cruz Biotechnology); anti-cytokeratin 7, rabbit monoclonal IgG (1:50, SP52, Ventana Medical Systems); anti-Ki67 (1:75, SP6, Thermo Fisher Scientific); anti-cleaved caspase 3 (1:150, D3E9, Cell Signaling Technology); anti-vimentin (1:100, D21H3, Cell Signaling Technology); anti-BrdU (1:1000, Bu20a, Cell Signaling Technology). Following overnight incubation, sections and coverslips were washed with PBS and incubated with Alexa Fluor goat anti-rabbit 488/568 and goat anti-mouse 488/568 conjugated secondary antibodies (Life Technologies) for 1 h at RT, washed in PBS and mounted using ProLong Gold mounting media containing DAPI (Life Technologies).

Slides were imaged using an AxioObserver inverted microscope (Carl Zeiss) using 20× Plan-Apochromat/0.80NA or 40× Plan-Apochromat oil/1.4NA objectives (Carl Zeiss). An ApoTome.2 structured illumination device (Carl Zeiss) set at full z-stack mode and five phase images was used for image acquisition. For quantification of BrdU signal in column trophoblasts, 2-4 cell columns per explant (n=9; obtained using a 20× objective) were used to calculate values; BrdU$^+$ cell proportions were calculated by BrdU/KRT7$^+$ cells per column; BrdU fluorescence intensity thresholds were used to calculate BrdU proportions within Matrigel explant columns. Images were obtained using an Axiocam 506 monochrome digital camera and processed and analyzed using ZenPro software (Carl Zeiss).

Immunohistochemistry

Decidua (10 weeks' gestation; n=1) from a first trimester pregnancy was fixed in 2% paraformaldehyde for 24 h at 4°C, paraffin embedded and serially sectioned at 6 µm onto glass slides. Heat-induced antigen retrieval was performed using sodium citrate [10 mM (pH 6.0)] followed by quenching endogenous peroxidases with 3% hydrogen peroxide for 30 min at RT. Sections were then permeabilized with 0.2% Triton-X-100 for 5 min at RT. Serum block was performed with 5% bovine serum albumin in tris-buffered saline with 0.05% Tween 20 (TBST). Sections were then incubated with mouse monoclonal HLA-G (1:100, clone 4H84, ExBio) diluted in TBST overnight at 4°C. Following overnight incubation, sections were incubated with Envision+ Dual Link Mouse/Rabbit HRP-linked secondary antibody (DAKO) for 1 h at RT. IgG1 isotype controls and secondary antibody-only negative controls were performed to confirm antibody specificity. Staining was developed via 3,3′-diaminobenzidine (DAB) chromogen (DAB Substrate Kit, Thermo Fisher Scientific), counterstained in Modified Harris Hematoxylin Solution (Sigma-Aldrich) and coverslips were mounted with Entellan mounting medium (Electron Microscopy Sciences).

RNAScope

RNA *in situ* hybridization was performed using RNAscope® 2.5 HD Assay-RED [Advanced Cell Diagnostics (ACD)] following the manufacturer's instructions (Wang et al., 2012). Briefly, placenta (n=3; 6-8 weeks' gestation) and Matrigel-embedded placental explants (n=15; five explants per oxygen condition) from first trimester pregnancies were fixed overnight at 4°C in 4% paraformaldehyde and paraffin-embedded. Tissue sections were serially sectioned at 6 µm and, following deparaffinization, antigen retrieval was performed using RNAscope® Target Retrieval Reagent (95°C for 15 min) and ACD Protease Plus Reagent (40°C for 30 min). RNAScope probes targeting LOX (Hs-LOX-C2; 415941-C2) and negative control (Probe-dapB; 310043) were incubated on sections for 2 h at 40°C and, following this, the RNAscope signal was amplified over six rounds of ACD AMP 1-6 incubation and application of RED-A and RED-B at a ratio of 1 volume of RED-B to 60 volumes of RED-A for 10 min at RT. Selected samples were counterstained with 50% Haematoxylin I for 2 min at RT and all samples were mounted using EcoMount (Biocare Medical).

Whole-mount hypoxia fluorescence imaging

Placental explants derived from 5- to 8-week-old gestation placentas (n=3) were established overnight at 5% oxygen as described above. Following establishment and verification of outgrowth by light microscopy, explants were cultured for an additional 24 h in either 1% or 20% oxygen. During the final 6 h of culture in either 1% or 20% oxygen, explant media was replaced with media containing 10 µM of Image-iT Green Hypoxia Reagent (an irreversible hypoxia sensing probe; Thermo Fisher Scientific) (Ayuso et al., 2016) for 2 h and, following this, media was replaced with regular explant media for the remaining 4 h. Upon completion of culture, placental explants were fixed in 4% paraformaldehyde for 30 min at RT, incubated with Hoechst 33258 nuclear stain (Thermo Fisher Scientific) and imaged with an AxioObserver inverted microscope (Carl Zeiss) using a 20× Plan-Apochromat/0.80NAobjective (Carl Zeiss).

RNA purification

Total RNA was prepared from column and invasive EVT cells using TRIzol reagent (Life Technologies) followed by RNeasy MinElute Cleanup (Qiagen) and DNase treatment (Life Technologies) according to the manufacturer's instructions. Care was taken so that explants were exposed to atmospheric oxygen for no longer than 2 min during microscopic dissection and separation of placental villi away from columns before the addition of TRIzol. RNA purity was confirmed using a NanoDrop Spectrophotometer (Thermo Fisher Scientific) and by running RNA samples on an Agilent

Development (2020) 147, dev181263. doi:10.1242/dev.181263

2100 Bioanalyzer (Agilent Technologies). Only RNA samples having an RNA integrity number (RIN)>8.0 were used.

Microarray hybridization, gene array data preprocessing and gene expression analysis

Total RNA samples extracted from explant columns were sent to Génome Québec Innovation Centre (McGill University, Montréal, Canada) for RNA quantification. Briefly, RNA samples were prepared for transcriptome profiling using the GeneChip™ Pico Reagent Kit (Thermo Fisher Scientific) as per the manufacturer's protocol. Samples were run on the Clariom™ S Human Array to measure gene expression at >20,000 genes in the human genome (Affymetrix). Raw data generated from the arrays were read into R statistical software (version 3.5.1) with the Bioconductor 'oligo' package to convert raw Affymetrix CEL files into an expression matrix of intensity values. The expression data was background corrected, Quantile normalized and log-transformed. A total of 13,787 control, duplicated, non-annotated or low intensity probes were filtered out of the data, leaving 13,402 probes for further analysis. Pre-processing was monitored at each step using principal component analysis (PCA) and linear modelling. PCA was performed by the `svd()` function from the `sva` package in R. Linear modelling was conducted using the R package limma. Probe-wise variances were shrunk using empirical Bayes with the `eBayes` function, followed by FDR adjustment for multiple testing (Benjamini and Hochberg, 1995). Differentially expressed genes were defined based on an FDR<0.05. Enrichment of pathways were identified and annotated using the clusterProfiler package in Bioconductor (Carvalho and Irizarry, 2010). Volcano plots were generated using the ggplot2 package for RStudio. Cluster analysis of sample relations based on principal components was generated using the `plotSampleRelation` function for the Lumi package. A hierarchical cluster analysis was conducted using Euclidean distances on the top 40 differentially expressed genes, selected by FDR<0.05 and ranked by fold-change>1.5.

Single cell RNA-seq data analysis

Processed droplet-based and Smart-seq2 single cell RNA sequencing data was obtained from public repositories (ArrayExpress experiment codes E-MTAB-6701 and E-MTAB-6678; Vento-Tormo et al., 2018). Cells belonging to clusters from trophoblast lineages (n=14,366) were merged from droplet-based and Smart-seq2 data, and corrected for batch-effects using canonical correlation analysis implemented in the R package Seurat (Butler et al., 2018). Pseudotime trajectory modelling was conducted using the monocle 2 R package (Qiu et al., 2017; Trapnell et al., 2014) under the recommended unsupervized procedure called 'dpFeature'. Briefly, the first 10 principal components on log-normalized expression data were used to construct a t-distributed stochastic neighbour embedding projection, upon which density-peak clustering determined 13 clusters, using the parameters rho=2, delta=10. The top 1000 differentially expressed genes between these clusters were then used for ordering the cells. Oxygen concentration-dependent genes were visualized along the inferred pseudotime-ordered branches using the R function 'monocle::plot_genes_branched_heatmap' with the following settings: the number of clusters k=5 for clustering the genes, and default parameters for everything else.

LOX activity assay, LOX inhibition and LOX siRNA knock-down

Measurement of endogenous LOX activity in placental explant CM was performed following a modified protocol described in Wiel et al. (2013). Briefly, 600 µl of CM from placental explants cultured in triplicate from either 1%, 5% or 20% oxygen conditions was pooled, concentrated 12-fold using 7.5 kDa exclusion Amicon Millipore concentration columns and snap-frozen in liquid nitrogen. LOX activity in 15 µl of concentrated CM was determined using the Amplex Red H_2O_2 detection kit following the manufacturer's instructions (Life Technologies). This assay is based on the ability of endogenous LOX to oxidize 10 mM 1,5-diaminopentane (DAP; a LOX substrate) in the presence of 0.5 U/ml horseradish peroxidase; the reaction was incubated at 37°C for 30 min. Oxidation of Amplex Red generates a fluorescence signal measurable at 560 nm/590 nm excitation/emission wavelengths and was detected using a fluorescence plate reader (BMG Labtech) using a 96-well format. As a positive control, 10 µg/ml recombinant active LOX (MyBioscource.com) was separately incubated with DAP substrate. LOX activity/specificity was determined by co-incubating reactions with 5 mM of BAPN. For endogenous inhibition of LOX within explant cultures, two approaches were used: LOX inhibition with BAPN, and LOX knockdown using LOX-specific siRNA. Following 24 h of explant establishment at 37°C, 5% CO_2, 5% O_2 in a humidified trigas incubator, explant media was replaced with media containing 500 µM of BAPN and explant cultures were placed into 1% or 20% O_2 culture conditions for an additional 48 h of culture before being imaged and measured. In control cultures, 0.5% DMSO (BAPN was solubilized in DMSO) was added to explant media. For siRNA delivery into explant cultures, 1 µM of Accell SMARTpool Human LOX siRNA (4015) was added directly to explants cultured in 1% or 20% oxygen via culture media. 1 µM Accell Human Control siRNA (K-005000-R1-01) was used as control non-silencing siRNA in these experiments. Following 72 h of culture, placental villi were dissected away from columns and the remaining column trophoblasts and matrix-invading EVT were recovered from Matrigel using Cell Recovery Solution (BD Biosciences), pelleted by centrifugation (300 ***g***) and washed in ice-cold PBS. Cells recovered from explants cultured in triplicate were pooled (~150,000 cells) and used for downstream immunoblot analyses.

Cell lysis and immunoblot analysis

Cells were washed in ice-cold PBS and incubated in RIPA cell extraction buffer [20 mM Tris-HCl (pH 7.6), 1% Triton X-100, 0.1% SDS, 1% NP-40, 1% sodium deoxycholate, 5 mM EDTA, 50 mM NaCl] supplemented with 10 mM Na_3VO_4, 10 mM NaF, 2 mM PMSF and an appropriate dilution of cOmplete Mini, EDTA-free protease inhibition cocktail tablets (Roche). Protein concentrations were determined using a BCA kit (Thermo Fisher Scientific). For immunoblotting, 10 µg of cell protein lysate was resolved by SDS-PAGE and transferred to nitrocellulose membranes. The membranes were probed using rabbit polyclonal antibodies directed against LOX (1:1000, NB100-2530SS, Novus Biologicals), or monoclonal antibodies directed against EGFR (1:2000, D38B1,Cell Signaling Technology), α-5 integrin (1:2000, D7B7G, Cell Signaling Technology) and HLA-G (1:2000, 4H84, Exbio). The blots were stripped and re-probed with an HRP-conjugated monoclonal antibody directed against mouse β-actin (1:5000, Santa Cruz Biotechnology).

BrdU incorporation assay

Pulse-chase labelling with BrdU (Sigma-Aldrich) was conducted on a verification cohort of Matrigel-embedded placental explants (n=3 distinct placentae, 4-11 columns per oxygen condition). Explants were established in 5% oxygen for 24 h followed by 24 h of culture in either 1%, 5% or 20% oxygen. After 48 h of culture, explants were exposed to a 4 h pulse with CM containing 10 µM of BrdU. Following 4 h of labelling, explants were washed in PBS and fixed in 4% paraformaldehyde overnight. Explants were paraffin embedded and sectioned for immunofluorescence microscopy. Immunofluorescent staining with anti-BrdU antibody (1:200, Bu20a, Sigma-Aldrich) was carried out with the addition of a 30-min incubation in 2 M HCl between permeabilization and sodium borohydride steps.

Statistical analysis

Data are reported as median values with standard deviations. All calculations were carried out using GraphPad Prism software. For single comparisons, Mann–Whitney non-parametric unpaired t-tests were performed. For multiple comparisons, one-way Kruskal–Wallis ANOVA followed by Dunn's multiple comparison test was performed on explant outgrowth data, as outgrowth in 1% oxygen was not normally distributed. One-way ANOVA followed by Tukey post-test were performed for all other multiple comparisons. The differences were accepted as significant at P<0.05. For gene microarray and scRNA-seq statistical analyses, please refer to the gene array data preprocessing and scRNA-seq analysis sections in the Materials and methods.

Acknowledgements

The authors extend their sincere gratitude to the hard work of staff at British Columbia's Women's Hospital's CARE Program for recruiting participants to our study, and thank Dr Megan K. Barker for her critical readings of the manuscript.

Competing interests
The authors declare no competing or financial interests.

Author contributions
Conceptualization: A.G.B.; Methodology: J.T., V.Y., J.B., H.T.L., B.C., A.G.B.; Software: V.Y.; Formal analysis: J.T., V.Y., J.B., H.T.L., B.C., A.G.B.; Investigation: J.T., V.Y., A.G.B.; Resources: W.P.R., A.G.B.; Writing - original draft: J.T., V.Y., W.P.R., A.G.B.; Writing - review & editing: J.T., V.Y., J.B., H.T.L., B.C., W.P.R., A.G.B.; Supervision: A.G.B.; Project administration: A.G.B.; Funding acquisition: A.G.B.

Funding
This work was supported by a Natural Sciences and Engineering Research Council of Canada Discovery Grant (NSERC; RGPIN-2014-04466 to A.G.B.), Canadian Institutes of Health Research operating grants (CIHR; 201403MOP-325905 and 201809PJT-407571-CIA-CAAA to A.G.B.) and a CIHR Master's graduate studentship (to J.T.).

Data availability
The data reported in this paper have been deposited in GEO under accession number GSE132421.

Supplementary information
Supplementary information available online at
http://dev.biologists.org/lookup/doi/10.1242/dev.181263.supplemental

References

Aghababaei, M., Perdu, S., Irvine, K. and Beristain, A. G. (2014). A disintegrin and metalloproteinase 12 (ADAM12) localizes to invasive trophoblast, promotes cell invasion and directs column outgrowth in early placental development. *Mol. Hum. Reprod.* **20**, 235-249. doi:10.1093/molehr/gat084

Aghababaei, M., Hogg, K., Perdu, S., Robinson, W. P. and Beristain, A. G. (2015). ADAM12-directed ectodomain shedding of E-cadherin potentiates trophoblast fusion. *Cell Death Differ.* **22**, 1970-1984. doi:10.1038/cdd.2015.44

Ashton, S. V., Whitley, G. S. J., Dash, P. R., Wareing, M., Crocker, I. P., Baker, P. N. and Cartwright, J. E. (2005). Uterine spiral artery remodeling involves endothelial apoptosis induced by extravillous trophoblasts through Fas/FasL interactions. *Arterioscler. Thromb. Vasc. Biol.* **25**, 102-108. doi:10.1161/01.ATV.0000148547.70187.89

Avagliano, L., Marconi, A. M., Romagnoli, S. and Bulfamante, G. P. (2012). Abnormal spiral arteries modification in stillbirths: the role of maternal prepregnancy body mass index. *J. Matern. Fetal. Neonatal. Med.* **25**, 2789-2792. doi:10.3109/14767058.2012.705395

Ayuso, J. M., Virumbrales-Muñoz, M., Lacueva, A., Lanuza, P. M., Checa-Chavarria, E., Botella, P., Fernández, E., Doblare, M., Allison, S. J., Phillips, R. M. et al. (2016). Development and characterization of a microfluidic model of the tumour microenvironment. *Sci. Rep.* **6**, 36086. doi:10.1038/srep36086

Barghash, A. and Arslan, T. (2016). Robust detection of outlier samples and genes in expression datasets. *J. Proteomics Bioinform.* **9**, 1-11. doi:10.4172/jpb.1000387

Benjamini, Y. and Hochberg, Y. (1995). Controlling the false discovery rate: a practical and powerful approach to multiple testing. *J. R. Stat. Soc. B Methodol.* **57**, 289-300. doi:10.1111/j.2517-6161.1995.tb02031.x

Bilban, M., Haslinger, P., Prast, J., Klinglmüller, F., Woelfel, T., Haider, S., Sachs, A., Otterbein, L. E., Desoye, G., Hiden, U. et al. (2009). Identification of novel trophoblast invasion-related genes: heme oxygenase-1 controls motility via peroxisome proliferator-activated receptor gamma. *Endocrinology* **150**, 1000-1013. doi:10.1210/en.2008-0456

Butler, A., Hoffman, P., Smibert, P., Papalexi, E. and Satija, R. (2018). Integrating single-cell transcriptomic data across different conditions, technologies, and species. *Nat. Biotechnol.* **36**, 411-420. doi:10.1038/nbt.4096

Caniggia, I., Mostachfi, H., Winter, J., Gassmann, M., Lye, S. J., Kuliszewski, M. and Post, M. (2000). Hypoxia-inducible factor-1 mediates the biological effects of oxygen on human trophoblast differentiation through TGFbeta(3). *J. Clin. Invest.* **105**, 577-587. doi:10.1172/JCI8316

Carvalho, B. S. and Irizarry, R. A. (2010). A framework for oligonucleotide microarray preprocessing. *Bioinformatics* **26**, 2363-2367. doi:10.1093/bioinformatics/btq431

Chakraborty, D., Rumi, M. A. K., Konno, T. and Soares, M. J. (2011). Natural killer cells direct hemochorial placentation by regulating hypoxia-inducible factor dependent trophoblast lineage decisions. *Proc. Natl. Acad. Sci. USA* **108**, 16295-16300. doi:10.1073/pnas.1109478108

Chakraborty, D., Cui, W., Rosario, G. X., Scott, R. L., Dhakal, P., Renaud, S. J., Tachibana, M., Rumi, M. A. K., Mason, C. W., Krieg, A. J. et al. (2016). HIF-KDM3A-MMP12 regulatory circuit ensures trophoblast plasticity and placental adaptations to hypoxia. *Proc. Natl. Acad. Sci. USA* **113**, E7212-E7221. doi:10.1073/pnas.1612626113

Chang, C.-W., Wakeland, A. K. and Parast, M. M. (2018). Trophoblast lineage specification, differentiation and their regulation by oxygen tension. *J. Endocrinol.* **236**, R43-R56. doi:10.1530/JOE-17-0402

Cowden Dahl, K. D., Fryer, B. H., Mack, F. A., Compernolle, V., Maltepe, E., Adelman, D. M., Carmeliet, P. and Simon, M. C. (2005). Hypoxia-inducible factors 1alpha and 2alpha regulate trophoblast differentiation. *Mol. Cell. Biol.* **25**, 10479-10491. doi:10.1128/MCB.25.23.10479-10491.2005

Cox, T. R., Rumney, R. M. H., Schoof, E. M., Perryman, L., Høye, A. M., Agrawal, A., Bird, D., Latif, N. A., Forrest, H., Evans, H. R. et al. (2015). The hypoxic cancer secretome induces pre-metastatic bone lesions through lysyl oxidase. *Nature* **522**, 106-110. doi:10.1038/nature14492

De Luca, L. C., Le, H. T., Mara, D. L. and Beristain, A. G. (2017). ADAM28 localizes to HLA-G(+) trophoblasts and promotes column cell outgrowth. *Placenta* **55**, 71-80. doi:10.1016/j.placenta.2017.05.009

Davies, J. E., Pollheimer, J., Yong, H. E. J., Kokkinos, M. I., Kalionis, B., Knöfler, M. and Murthi, P. (2016). Epithelial-mesenchymal transition during extravillous trophoblast differentiation. *Cell Adh. Migr.* **10**, 310-321. doi:10.1080/19336918.2016.1170258

Di Stefano, V., Torsello, B., Bianchi, C., Cifola, I., Mangano, E., Bovo, G., Cassina, V., De Marco, S., Corti, R., Meregalli, C. et al. (2016). Major action of endogenous lysyl oxidase in clear cell renal cell carcinoma progression and collagen stiffness revealed by primary cell cultures. *Am. J. Pathol.* **186**, 2473-2485. doi:10.1016/j.ajpath.2016.05.019

Farrell, A., Alahari, S., Ermini, L., Tagliaferro, A., Litvack, M., Post, M. and Caniggia, I. (2019). Faulty oxygen sensing disrupts angiomotin function in trophoblast cell migration and predisposes to preeclampsia. *JCI Insight* **4**, 127009. doi:10.1172/jci.insight.127009

Fock, V., Plessl, K., Draxler, P., Otti, G. R., Fiala, C., Knöfler, M. and Pollheimer, J. (2015a). Neuregulin-1-mediated ErbB2-ErbB3 signalling protects human trophoblasts against apoptosis to preserve differentiation. *J. Cell. Sci.* **128**, 4306-4316. doi:10.1242/jcs.176933

Fock, V., Plessl, K., Fuchs, R., Dekan, S., Milla, S. K., Haider, S., Fiala, C., Knöfler, M. and Pollheimer, J. (2015b). Trophoblast subtype-specific EGFR/ERBB4 expression correlates with cell cycle progression and hyperplasia in complete hydatidiform moles. *Hum. Reprod.* **30**, 789-799. doi:10.1093/humrep/dev027

Genbacev, O., Zhou, Y., Ludlow, J. W. and Fisher, S. J. (1997). Regulation of human placental development by oxygen tension. *Science* **277**, 1669-1672. doi:10.1126/science.277.5332.1669

Gultice, A. D., Kulkarni-Datar, K. and Brown, T. L. (2009). Hypoxia-inducible factor 1alpha (HIF1A) mediates distinct steps of rat trophoblast differentiation in gradient oxygen. *Biol. Reprod.* **80**, 184-193. doi:10.1095/biolreprod.107.067488

Haider, S., Meinhardt, G., Saleh, L., Fiala, C., Pollheimer, J. and Knöfler, M. (2016). Notch1 controls development of the extravillous trophoblast lineage in the human placenta. *Proc. Natl. Acad. Sci. USA* **113**, E7710-E7719. doi:10.1073/pnas.1612335113

Haider, S., Meinhardt, G., Saleh, L., Kunihs, V., Gamperl, M., Kaindl, U., Ellinger, A., Burkard, T. R., Fiala, C., Pollheimer, J. et al. (2018). Self-renewing trophoblast organoids recapitulate the developmental program of the early human placenta. *Stem Cell Rep.* **11**, 537-551. doi:10.1016/j.stemcr.2018.07.004

Horii, M., Li, Y., Wakeland, A. K., Pizzo, D. P., Nelson, K. K., Sabatini, K., Laurent, L. C., Liu, Y. and Parast, M. M. (2016). Human pluripotent stem cells as a model of trophoblast differentiation in both normal development and disease. *Proc. Natl. Acad. Sci. USA* **113**, E3882-E3891. doi:10.1073/pnas.1604747113

James, J. L., Stone, P. R. and Chamley, L. W. (2006). The effects of oxygen concentration and gestational age on extravillous trophoblast outgrowth in a human first trimester villous explant model. *Hum. Reprod.* **21**, 2699-2705. doi:10.1093/humrep/del212

Jauniaux, E., Watson, A., Ozturk, O., Quick, D. and Burton, G. (1999). *In-vivo* measurement of intrauterine gases and acid-base values early in human pregnancy. *Human Reprod.* **14**, 2901-2904. doi:10.1093/humrep/14.11.2901

Jauniaux, E., Kiserud, T., Ozturk, O., West, D. and Hanson, M. A. (2000). Amniotic gas values and acid-base status during acute maternal hyperoxemia and hypoxemia in the early fetal sheep. *YMOB* **182**, 661-665. doi:10.1067/mob.2000.103937

Jauniaux, E., Watson, A. and Burton, G. (2001). Evaluation of respiratory gases and acid-base gradients in human fetal fluids and uteroplacental tissue between 7 and 16 weeks' gestation. *YMOB* **184**, 998-1003. doi:10.1067/mob.2001.111935

Kabir-Salmani, M., Shiokawa, S., Akimoto, Y., Sakai, K. and Iwashita, M. (2004). The role of alpha(5)beta(1)-integrin in the IGF-I-induced migration of extravillous trophoblast cells during the process of implantation. *Mol. Hum. Reprod.* **10**, 91-97. doi:10.1093/molehr/gah014

Keogh, R. J., Harris, L. K., Freeman, A., Baker, P. N., Aplin, J. D., Whitley, G. S. J. and Cartwright, J. E. (2007). Fetal-derived trophoblast use the apoptotic cytokine tumor necrosis factor-alpha-related apoptosis-inducing ligand to induce smooth muscle cell death. *Circ. Res.* **100**, 834-841. doi:10.1161/01.RES.0000261352.81736.37

Kim, S. N., Jeibmann, A., Halama, K., Witte, H. T., Wälte, M., Matzat, T., Schillers, H., Faber, C., Senner, V., Paulus, W. et al. (2014). ECM stiffness regulates glial

migration in Drosophila and mammalian glioma models. *Development* **141**, 3233-3242. doi:10.1242/dev.106039

Lash, G. E., Otun, H. A., Innes, B. A., Bulmer, J. N., Searle, R. F. and Robson, S. C. (2006). Low oxygen concentrations inhibit trophoblast cell invasion from early gestation placental explants via alterations in levels of the urokinase plasminogen activator system. *Biol. Reprod.* **74**, 403-409. doi:10.1095/biolreprod.105.047332

Maltepe, E., Krampitz, G. W., Okazaki, K. M., Red-Horse, K., Mak, W., Simon, M. C. and Fisher, S. J. (2005). Hypoxia-inducible factor-dependent histone deacetylase activity determines stem cell fate in the placenta. *Development* **132**, 3393-3403. doi:10.1242/dev.01923

Newby, D., Marks, L., Cousins, F., Duffie, E. and Lyall, F. (2005). Villous explant culture: characterization and evaluation of a model to study trophoblast invasion. *Hypertens. Pregnancy* **24**, 75-91. doi:10.1081/PRG-45785

Okae, H., Toh, H., Sato, T., Hiura, H., Takahashi, S., Shirane, K., Kabayama, Y., Suyama, M., Sasaki, H. and Arima, T. (2018). Derivation of human trophoblast stem cells. *Cell Stem Cell* **22**, 50-63.e6. doi:10.1016/j.stem.2017.11.004

Perdu, S., Castellana, B., Kim, Y., Chan, K., DeLuca, L. and Beristain, A. G. (2016). Maternal obesity drives functional alterations in uterine NK cells. *JCI Insight* **1**, e85560. doi:10.1172/jci.insight.85560

Pijnenborg, R., Vercruysse, L. and Carter, A. M. (2011). Deep trophoblast invasion and spiral artery remodelling in the placental bed of the chimpanzee. *Placenta* **32**, 400-408. doi:10.1016/j.placenta.2011.02.009

Pollheimer, J., Vondra, S., Baltayeva, J., Beristain, A. G. and Knöfler, M. (2018). Regulation of placental extravillous trophoblasts by the maternal uterine environment. *Front. Immunol.* **9**, 2597. doi:10.3389/fimmu.2018.02597

Qiu, X., Mao, Q., Tang, Y., Wang, L., Chawla, R., Pliner, H. A. and Trapnell, C. (2017). Reversed graph embedding resolves complex single-cell trajectories. *Nat. Methods* **14**, 979-982. doi:10.1038/nmeth.4402

Robins, J. C., Heizer, A., Hardiman, A., Hubert, M. and Handwerger, S. (2007). Oxygen tension directs the differentiation pathway of human cytotrophoblast cells. *Placenta* **28**, 1141-1146. doi:10.1016/j.placenta.2007.05.006

Rodesch, F., Simon, P., Donner, C. and Jauniaux, E. (1992). Oxygen measurements in endometrial and trophoblastic tissues during early pregnancy. *Obstet. Gynecol.* **80**, 283-285.

Segond, N., Degrelle, S. A., Berndt, S., Clouqueur, E., Rouault, C., Saubamea, B., Dessen, P., Fong, K. S. K., Csiszar, K., Badet, J. et al. (2013). Transcriptome analysis of PPARγ target genes reveals the involvement of lysyl oxidase in human placental cytotrophoblast invasion. *PLoS ONE* **8**, e79413. doi:10.1371/journal.pone.0079413

Tilburgs, T., Crespo, Â. C., van der Zwan, A., Rybalov, B., Raj, T., Stranger, B., Gardner, L., Moffett, A. and Strominger, J. L. (2015a). Human HLA-G+ extravillous trophoblasts: Immune-activating cells that interact with decidual leukocytes. *Proc. Natl. Acad. Sci. USA* **112**, 7219-7224. doi:10.1073/pnas.1507977112

Tilburgs, T., Evans, J. H., Crespo, Â. C. and Strominger, J. L. (2015b). The HLA-G cycle provides for both NK tolerance and immunity at the maternal-fetal interface. *Proc. Natl. Acad. Sci. USA* **112**, 13312-13317. doi:10.1073/pnas.1517724112

Trapnell, C., Cacchiarelli, D., Grimsby, J., Pokharel, P., Li, S., Morse, M., Lennon, N. J., Livak, K. J., Mikkelsen, T. S. and Rinn, J. L. (2014). The dynamics and regulators of cell fate decisions are revealed by pseudotemporal ordering of single cells. *Nat. Biotechnol.* **32**, 381-386. doi:10.1038/nbt.2859

Turco, M. Y., Gardner, L., Kay, R. G., Hamilton, R. S., Prater, M., Hollinshead, M. S., McWhinnie, A., Esposito, L., Fernando, R., Skelton, H. et al. (2018). Trophoblast organoids as a model for maternal-fetal interactions during human placentation. *Nature* **564**, 263-267. doi:10.1038/s41586-018-0753-3

Velicky, P., Knöfler, M. and Pollheimer, J. (2016). Function and control of human invasive trophoblast subtypes: Intrinsic vs. maternal control. *Cell Adh. Migr.* **10**, 154-162. doi:10.1080/19336918.2015.1089376

Velicky, P., Meinhardt, G., Plessl, K., Vondra, S., Weiss, T., Haslinger, P., Lendl, T., Aumayr, K., Mairhofer, M., Zhu, X. et al. (2018). Genome amplification and cellular senescence are hallmarks of human placenta development. *PLoS Genet.* **14**, e1007698. doi:10.1371/journal.pgen.1007698

Vento-Tormo, R., Efremova, M., Botting, R. A., Turco, M. Y., Vento-Tormo, M., Meyer, K. B., Park, J.-E., Stephenson, E., Polański, K., Goncalves, A. et al. (2018). Single-cell reconstruction of the early maternal-fetal interface in humans. *Nature* **563**, 347-353. doi:10.1038/s41586-018-0698-6

Wakeland, A. K., Soncin, F., Moretto-Zita, M., Chang, C.-W., Horii, M., Pizzo, D., Nelson, K. K., Laurent, L. C. and Parast, M. M. (2017). Hypoxia directs human extravillous trophoblast differentiation in a hypoxia-inducible factor-dependent manner. *Am. J. Pathol.* **187**, 767-780. doi:10.1016/j.ajpath.2016.11.018

Wang, F., Flanagan, J., Su, N., Wang, L.-C., Bui, S., Nielson, A., Wu, X., Vo, H.-T., Ma, X.-J. and Luo, Y. (2012). RNAscope: a novel in situ RNA analysis platform for formalin-fixed, paraffin-embedded tissues. *J. Mol. Diagn.* **14**, 22-29. doi:10.1016/j.jmoldx.2011.08.002

Wiel, C., Augert, A., Vincent, D. F., Gitenay, D., Vindrieux, D., Le Calvé, B., Arfi, V., Lallet-Daher, H., Reynaud, C., Treilleux, I. et al. (2013). Lysyl oxidase activity regulates oncogenic stress response and tumorigenesis. *Cell Death Dis.* **4**, e855. doi:10.1038/cddis.2013.382

Xu, X.-H., Jia, Y., Zhou, X., Xie, D., Huang, X., Jia, L., Zhou, Q., Zheng, Q., Zhou, X., Wang, K. et al. (2019). Downregulation of lysyl oxidase and lysyl oxidase-like protein 2 suppressed the migration and invasion of trophoblasts by activating the TGF-β/collagen pathway in preeclampsia. *Exp. Mol. Med.* **51**, 20. doi:10.1038/s12276-019-0211-9

Zhou, Y., Fisher, S. J., Janatpour, M., Genbacev, O., Dejana, E., Wheelock, M. and Damsky, C. H. (1997). Human cytotrophoblasts adopt a vascular phenotype as they differentiate. A strategy for successful endovascular invasion? *J. Clin. Invest.* **99**, 2139-2151. doi:10.1172/JCI119387